Microwave Imaging Reflectometry (MIR) on the DIII-D tokamak

Benjamin Tobias, G.J. Kramer, and E. Valeo

Princeton Plasma Physics Laboratory
100 Stellarator Rd., Princeton, NJ, USA 08540
E-mail: bjtobias@pppl.gov

C.M. Muscatello*, X. Ren, M. Chen, A.G. Spear, A.-V. Pham, T. Phan, M. Mamidanna, J. Lai, M. Li, D. Fu, F. Hu, C.W. Domier, and N.C. Luhmann, Jr.

University of California at Davis
1 Shields Ave., Davis, CA, USA 95616

X. Chen, N. Ferraro, A. Garofalo

General Atomics*
3483 Dunhill St, San Diego, CA, USA 92121

S. Zemedkun and T.L. Munsat

University of Colorado at Boulder
830 UCB, Boulder, CO, USA 80309

Y. Zhu

University of Science and Technology, China
96 JinZhai Rd., Hefei, Anhui, PRC, 230026

Microwave Imaging Reflectometry (MIR) couples a multi-frequency illumination source to a shaped, 2D array of miniature, quasi-optical substrate lens antennas in order to provide a 2D image of the fluctuating electron density within a confined plasma. The successful implementation of this technique on the DIII-D tokamak is now entering its second year of operation and has obtained a wealth of previously unobtainable data pertaining to coherent modes and broadband turbulence in core and edge regions. The first measurements of 2D Alfvén eigenmode structure using this technique are presented. The poloidally spaced measurements provide the poloidal wavenumber and define a dispersion relationship for a spectrum of modes. This capability is shown to readily distinguish different eigenmodes and branches of instability, even when Doppler shift due to plasma rotation causes the observed frequencies to overlap. Furthermore, direct measurement of the poloidal propagation of unstable eigenmodes allows for comparison to the locally fitted plasma fluid rotation. This technique has been used to understand new measurements of edge harmonic oscillation (EHOs) thought to contribute to the formation of the so-called quiescent high-confinement mode, or QH-mode, on DIII-D. The incidence of diagnostic artifacts in the characterization of these long poloidal wavelengths is being explored in detail with synthetic diagnostic forward modeling techniques and the full-wave reflectometer codes FWR2D and FWR3D, revealing a correlation with non-idealities of mode structure. Planned diagnostic upgrades that will improve the quality of this data and allow for further investigation of ELM suppression and naturally ELM-free operating scenarios are also discussed.

1. Introduction

Microwave reflectometry is a radar-like technique that probes density dependent cutoff layers by transmitting a beam of radiation and collecting that radiation after reflection from the plasma. As in radar, the quality of the data collected depends on the quality of the reflection. In the idealized limit, the wave cutoff is like a planar mirror and the diagnostic collects a specular reflection at normal incidence. The time of flight or phase of the reflected wave is analyzed by the diagnostic to infer the position or perturbations on that 'mirror.' In practice, however, we are interested in cases where the reflecting layer can be quite complicated and the pattern of scattered waves may appear rather chaotic. Imaging collects this scattered radiation to form an image of the perturbed fields at the cutoff layer on an array of detectors, thereby restoring the perturbations of wave phase that are due to fluctuating density and magnetic field [1]. This is the cardinal advantage of imaging in reflectometry, and its application in a density fluctuation diagnostic provides a robust, spatially localized, 2D measurement of both turbulence and coherent mode structure.

The DIII-D MIR diagnostic [2] is installed at the 270R0 midplane port and views the same region of plasma as ECE-Imaging [3]. This allows for a simultaneous measurement of fluctuating electron temperature and density with comparable spatial resolution. Shared optical components were optimized to reduce aberration in ECE-Imaging while providing maximum plasma coverage. The imaging conditions for MIR are different, however, in that both the incident and reflected beams must be matched to the curvature of the density cutoff layer as closely as possible. Therefore, as shown in Figure 1, the MIR imaging array is curved in a manner that approximates the curvature of cutoff surfaces near the plasma edge.
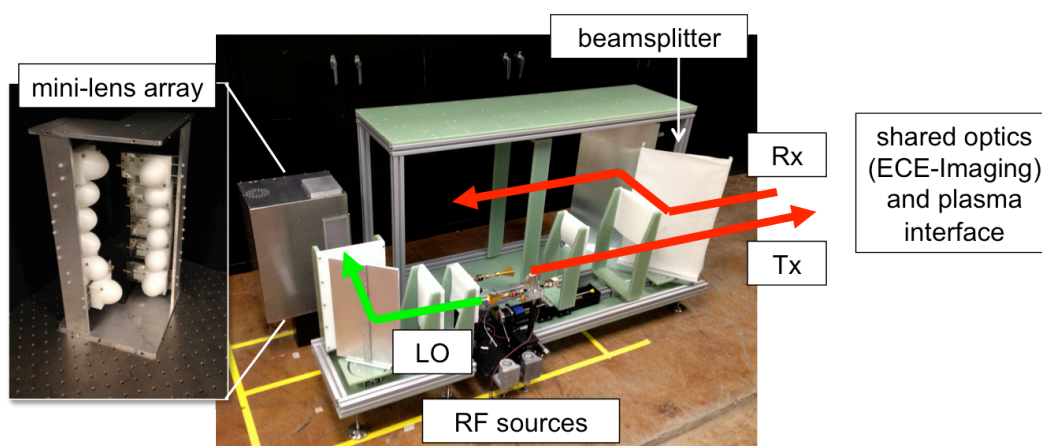
Figure 1. The modular layout of MIR-specific hardware and optics. Transmit and receive paths are combined at the beamsplitter shown and propagate through shared optics controlling vertical zoom and vacuum interface at the port window. Local oscillator power is coupled optically to the imaging array with collimating high-density polyethylene lenses. The miniature substrate lens array (left) is curved to facilitate curvature of the image plane and matching of the density cutoff layer.

In order to provide a 2D picture of fluctuating density, the DIII-D MIR diagnostic simultaneously probes the plasma with 4 frequencies [4]. The probe frequencies are generated by mixing with a 65 GHz fixed-frequency Gunn diode oscillator, as shown in Figure 2. The intermediate frequency, or IF, may be tuned over 2-8 GHz to probe density cutoff layers between 57 and 73 GHz. The signal that is reflected to the receiver array is mixed at the antenna (GaAs Schottky diode) with a local oscillator source offset by 370 MHz. The resultant IF is then mixed with local IF sources detuned by 510 MHz. This downconverts the probe frequencies to either 140 or 880 MHz, corresponding to either the upper or lower probe sideband. These are filtered and mixed with phase-locked 140 and 880 MHz local oscillator signals to produce the complex, i.e. in phase and quadrature, signal output. The phase of this complex output reflects the relative phase of transmit and receive waves at the detector, and therefore fluctuations in the reflecting layer.
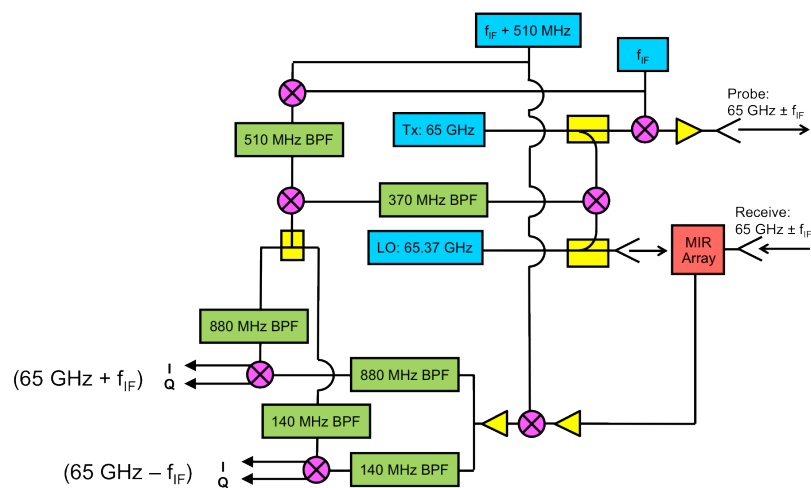
Figure 2. A block diagram of the multi-channel approach to fluctuation reflectometry adopted in the DIII-D MIR system. The downconverted IF spectrum is mixed with 880 and 140 MHz sources to isolate signals corresponding to the upper (RF+IF) and lower (RF-IF) reflectometer probe channels. During FY14, the DIII-D MIR system made use of two local IF sources, producing two pairs of independently tunable channels.

2. Imaging of reversed-shear-induced and toroidicity-induced Alfvén eigenmodes

Imaging of Alfvén eigenmodes demonstrates both the capabilities and current limitations of MIR. Alfvén eigenmodes on DIII-D exhibit characteristic frequencies and wavenumbers that are within the optimum range, and while data quality does not yet allow for extraction of meaningful 2D images in real time, we are able to estimate the 2D (frequency vs. wavenumber) power spectral density [5] over a given time and compare this with an idealized expectation. Figure 3 shows MIR data pertaining to the evolution of RSAE and TAE mode structure in time. L-mode is a particularly challenging scenario for MIR due to weak density gradients and elevated levels of turbulence, and the spread in wavenumber here is greater than that observed by ECE-Imaging [6]. However, both TAEs and RSAEs are detected, and one may directly observe that poloidal wavenumber remains relatively

constant as the RSAE frequency increases. This sweeping of the mode with evolution of the q-profile therefore results in an acceleration of the poloidal phase velocity that is consistent with theory [7].
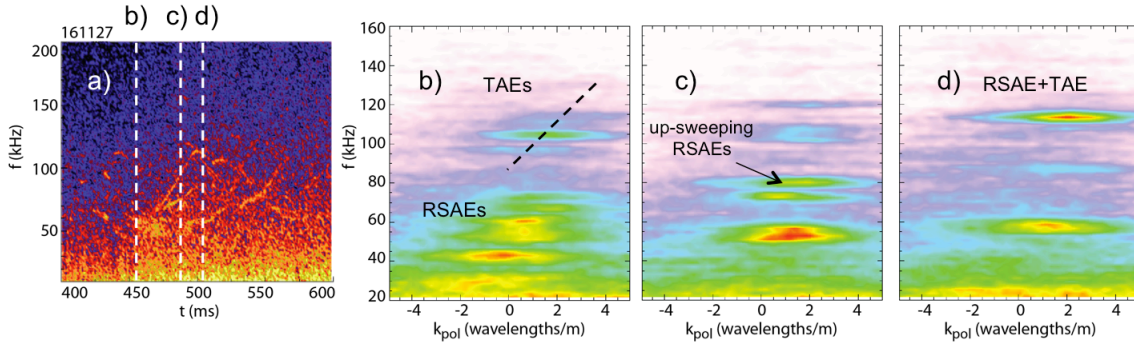

Figure 3. a) A single-channel spectrogram from MIR reveals a number of reversed-shear-induced Alfvén eigenmodes that sweep between 40 and 120 kHz as the safety factor, q, is varied during the L-mode phase of DIII-D discharge 161127. b) At 450 ms, both RSAEs and TAEs are observed by the diagnostic. Fitting a line through the spectrum of TAE modes provides an estimate of the Doppler shift and natural TAE frequency, i.e. the observed frequency in the absence of rotation. c) As q_{min} decreases, RSAEs sweep upward toward the TAE band. d) At the upper limit of their sweep, RSAEs couple to modes in the TAE gap.

3. Diagnosis of edge harmonic oscillations (EHOs) in quiescent H-mode regimes

The so-called QH-mode is under development at DIII-D and elsewhere as a potentially ITER-relevant, ELM-free operating regime [8]. In this scenario, a low-n perturbation, the coherent EHO, has been hypothesized to be destabilized by flow shear in the edge region and implicated in regulating the growth of the pedestal, thereby avoiding ELMs. However, the physics of this process are not well understood and require a validated model for the instability, its formation, saturation and structure. Figure 4 shows MIR data pertaining to an EHO with dominant n=1 and n=3 components.
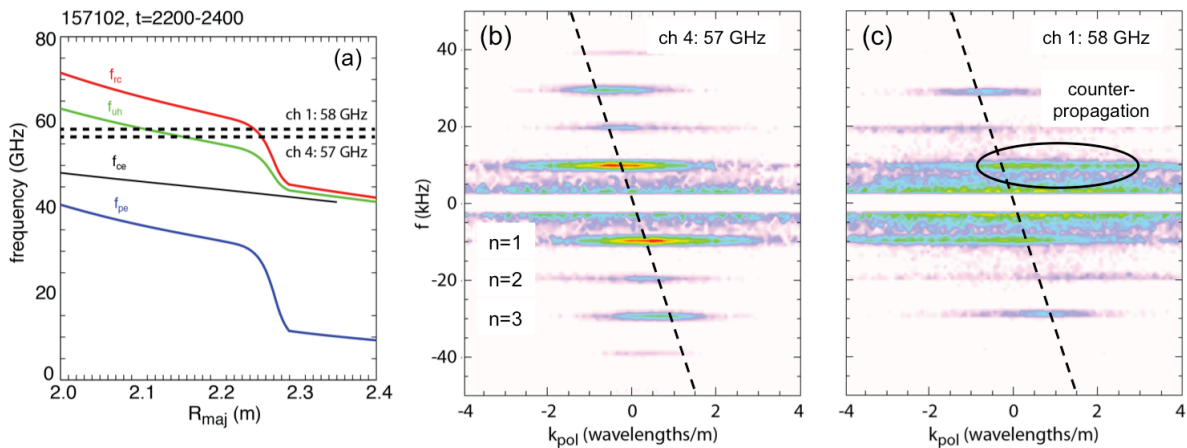

Figure 4. a) Characteristic frequencies for shot 157102. MIR channels 1 and 4 corresponding probe frequencies intersecting the plasma near the top of the H-mode pedestal and within the steep gradient

region. b) Channels that remain within the steep gradient region of the pedestal produce wavenumber spectra whose peaks correspond well to both Mirnov probe and ECE-Imaging data (for clarity, data below 4 kHz has been filtered from the image). c) Channels intersecting the top of the pedestal, however, indicate a counter-propagation of the local mode structure that likely reflects a diagnostic artifact. For reference, dashed lines indicate a poloidal velocity of 28 km/s.

Spanning only 19 vertical cm of plasma, the long poloidal wavelength of this mode, roughly 2 m, is near the resolution limits of MIR, and significant spread in detected wavenumber is expected. However, in some cases, MIR data suggests a counter-propagation, i.e. a reversal of the poloidal phase velocity at some radii. This is not corroborated by other diagnostics. However, it is reminiscent of a diagnostic artifact that is well-known and often seen in ECE-Imaging data [9]. There, it reflects the presence of a narrow inversion radius that is not perfectly aligned with a vertical row of channels. It remains to be seen if this is also the source of the artifact in MIR data, in which case it indicates an unexpected parity in the structure of the mode, possibly even a magnetic island near the top of the pedestal. Identification of such features, validated by synthetic diagnostic forward modeling, would be invaluable in comparison with MHD modeling. Forward modeling using the full-wave reflectometer codes FWR2D and FWR3D [10,11] is ongoing.

4. Future work and ongoing diagnostic development

The successful identification and characterization of poloidal mode structure validates the optical techniques applied in MIR. However, much work remains to improve signal-to-noise by improving the stability of heterodyning circuits and the available power from illumination and LO sources. Many sources of instability are inherent to the current implementation and require a combination of new technology and innovative system design. Figure 5 compares the existing heterodyne receiver configuration with the new approach that is being pursued.
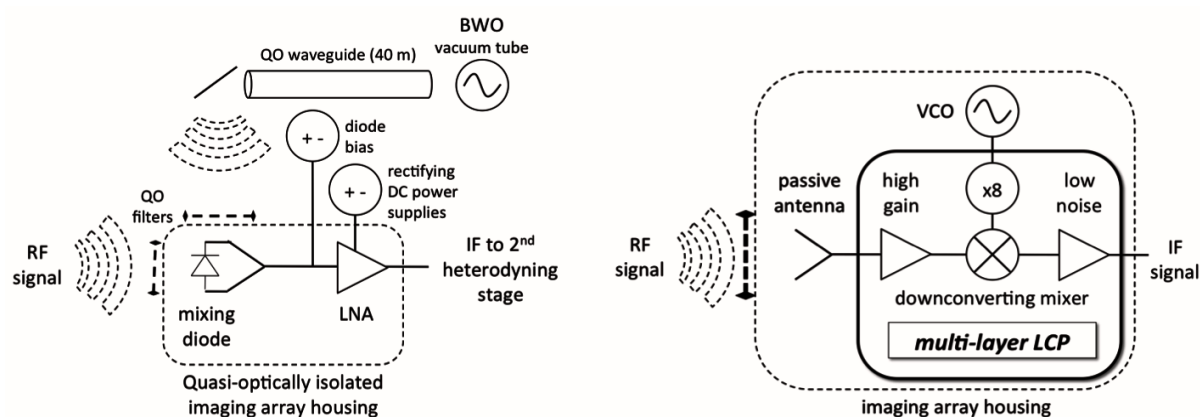

Figure 5. A block-diagram summarizing upgrades planned for MIR and ECE-Imaging receiver sub-system. Multiple sources of noise and instability may be overcome by eliminating optical coupling of the local oscillator, and with it both sensitivity to mechanical vibrations and the need for long runs of low-loss over-moded waveguide. Secondly, advances in microwave amplifier technology will soon allow the mixer to be placed after direct amplification at mm-wave frequencies for dramatically improved electromagnetic isolation and system noise temperature.

Electromagnetic shielding and isolation are improved by consolidating LO generation, deliver, and mixing on the same circuit and hermetically packaging these components. This also eliminates mechanically sensitive optical LO coupling, and the long runs of quasi-optical waveguide that are sometimes required. Furthermore, reversing the order of pre-amplification and mixing dramatically improves the overall system noise temperature [12]. These modifications are made possible by new technologies including, but not limited to, ultra-wideband CMOS amplifiers and the adoption of liquid crystal polymer (LCP) as a substrate for advanced mm-wave circuit design.

Acknowledgments

References

[1]   E. Mazzucato, et al., *Fluctuation measurements in tokamaks with microwave imaging reflectometry*, Phys. Plasmas **9**, 1955 (2002)

[2]   C.M. Muscatello, et al., *Technical overview of the millimeter-wave imaging reflecometer on the DIII-D tokamak*, Rev. Sci. Instrum. **85** 11D702 (2014)

[3]   B. Tobias, et. al. *Commisioning of electron cyclotron emission imaging on the DIII-D tokamak and first data*, Rev. Sci. Instrum. **81**, 10D928 (2010)

[4]   A. Spear, et al., *2D microwave imaging reflectometer electronics*, Rev. Sci. Instrum. **85**, 11D834 (2014)

[5]   J.M. Beall, Y.C. Kim and E.J. Powers, *Estimation of wavenumber and frequency spectra using fixed probe pairs*, Journal of Applied Physics **53**, 3933 (1982)

[6]   B. Tobias, et al., *Fast ion induced shearing of 2D Alfvén eigenmodes by electron cyclotron emission imaging*, Phys. Rev. Lett. **106**, 075003 (2011)

[7]   W. Deng, et al., *Linear properties of reversed shear Alfvén eigenmodes in the DIII-D tokamak*, Nuclear Fusion **52**, 043006 (2012)

[8]   A. Garofalo, et al., *Advances towards QH-mode viability for ELM-stable operation in ITER*, Nuclear Fusion **51**, 083018 (2011)

[9]   B. Tobias, et al., *ECE-Imaging of the H-mode pedestal*, Rev. Sci. Instrum. **83**, 10E329 (2012)

[10]   E.J. Valeo, G.J. Kramer, R. Nazikian, *Two-dimensional simulations of correlation reflectometry in fusion plasmas*, Plasma Phys. and Control. Fusion **44**, L1 (2002)

[11]   L. Lei, et al., *A synthetic diagnostic for the evaluation of new microwave imaging reflectometry diagnostics for DIII-D and KSTAR*, Rev. Sci. Instrum. **81**, 10D904 (2010)

[12]   J. Lai, C.W. Domier and N.C. Luhmann, Jr., *Noise temperature improvement for magnetic fusion plasma millimeter wave imaging systems*, Rev. Sci. Instrum. **85**, 033501 (2014)